NEUROSCIENCE

Egocentric coding of external items in the lateral entorhinal cortex

Cheng Wang[1]*, Xiaojing Chen[1]*, Heekyung Lee[1], Sachin S. Deshmukh[2], D. Yoganarasimha[3], Francesco Savelli[1], James J. Knierim[1,4]†

Episodic memory, the conscious recollection of past events, is typically experienced from a first-person (egocentric) perspective. The hippocampus plays an essential role in episodic memory and spatial cognition. Although the allocentric nature of hippocampal spatial coding is well understood, little is known about whether the hippocampus receives egocentric information about external items. We recorded in rats the activity of single neurons from the lateral entorhinal cortex (LEC) and medial entorhinal cortex (MEC), the two major inputs to the hippocampus. Many LEC neurons showed tuning for egocentric bearing of external items, whereas MEC cells tended to represent allocentric bearing. These results demonstrate a fundamental dissociation between the reference frames of LEC and MEC neural representations.

The hippocampus is critical for the formation and retrieval of episodic memories (*1*–*3*). Episodic memories preserve a person's original, first-person (i.e., egocentric) perspective (*4*). Cognitive map theory proposes that the hippocampus provides an objective spatial framework that is used to organize the various components of an experience, binding them so that they can be stored and later retrieved as a re-experience of the original event (*5*). Current theories propose that the various allocentric spatial correlates of cells in the hippocampus and MEC (*6*) provide the objective spatial framework of an experience. In contrast, representations of the specific components of an experience (i.e., the content) have been hypothesized to be provided by the LEC (*7*, *8*), in an egocentric framework (*9*).

We thus examined the behavior of 275 LEC cells while seven rats performed a foraging task in two-dimensional (2D) open arenas in which the walls or boundaries were the most prominent features of the local environment (Fig. 1A and fig. S1A). Although the firing rate maps of LEC cells showed weak spatial selectivity (*10*, *11*), some LEC cells showed activity patterns that suggested an egocentric representation of the nearby boundaries (*12*) or, equivalently, the center of the apparatus (Fig. 1, B to E, and figs. S2 and S3). We constructed tuning curves of the egocentric bearing (the angle of the vector from the rat to an external item, referenced from the allocentric head direction of the rat) of the nearest boundary ($Bearing_{Boundary}$) (Fig. 1B) (*13*, *14*) and compared them with classic allocentric head direction tuning curves (curves on right, Fig. 1, C, and E). LEC cells tended to have more sharply tuned egocentric bearing selectivity than head direction selectivity (Wilcoxon signed-rank test, z = 8.46, $P = 2.56 \times 10^{-17}$, n = 275) (Fig. 1F). Across the population with significant tuning, the preferred $Bearing_{Boundary}$ covered all angles, albeit nonuniformly, with an underrepresentation of 180° (fig. S4A). From these cells, it was possible to decode the $Bearing_{Boundary}$ of the rats throughout the session (fig. S4) (*15*). Egocentric bearing tuning was not an artifact of directional sampling biases, body-centered self-motion, or movement direction (fig. S5), and it was stable within a session (fig. S6). Some LEC cells showed tuning for distance of the animal to the boundary, and 23% of these cells showed $Bearing_{Boundary}$ selectivity as well (fig. S7 and table S1).

In contrast, $Bearing_{Boundary}$ tuning of MEC neurons recorded in the small-large box task (fig. S1B) was significantly weaker than that of LEC cells, as quantified by the mean vector length of the tuning curve ($MVL_{Boundary}$) (LEC median = 0.31, MEC median = 0.11; Wilcoxon rank-sum test, z = 6.84, $P = 8.0 \times 10^{-12}$; LEC, n = 72, MEC, n = 117) (Fig. 1, G and H, and fig. S8). Because some MEC neurons show conjunctive tuning for location and head direction (*6*), which could be confounded with $Bearing_{Boundary}$ tuning, we applied a generalized linear model (GLM) framework (*15*) (fig. S9) to dissociate an allocentric model (with a spatial location component conjunctive with allocentric bearing, i.e., classic head direction) from an egocentric model (with a spatial location component conjunctive with egocentric bearing). The goodness of fit was assessed with a Bayesian information criterion measure ($\Delta BIC_{Boundary}$)(*15*). A negative value of the $\Delta BIC_{Boundary}$ indicated that the egocentric model was a better fit than the allocentric model, and a positive value indicated the opposite. LEC and MEC cells were significantly better fit by the egocentric and the allocentric models, respectively (LEC median = −0.0076, MEC median = 0.0016; Wilcoxon signed-rank test; LEC: z = −6.44, $P = 1.22 \times 10^{-10}$, n = 72; MEC: z = 5.68, $P = 1.34 \times 10^{-8}$, n = 117; LEC vs. MEC: Wilcoxon rank-sum test, z = −8.88, $P = 6.46 \times 10^{-19}$) (Fig. 1I, fig. S10, and tables S1 to S3), revealing a double dissociation in the preferred reference frames for angular coordinates of LEC and MEC representations.

We constructed mean vector length (MVL) spatial maps to search for the location that generated the sharpest egocentric tuning curve [i.e., the largest MVL (MVL_{Max})] (Fig. 1J). For cells with tuning for the egocentric bearing of the boundary, the location that produces the MVL_{Max} will be at the center of the arena (fig. S2). The MVL_{Max} locations of LEC cells but not of MEC cells were significantly clustered around the center (Monte Carlo test for nonrandom distribution; LEC: $P < 0.001$, n = 72; MEC: P = 0.16, n = 117), with those of MEC cells significantly more scattered than those for LEC cells (bootstrap test, $P < 0.001$) (Fig. 1K and figs. S3 and S8). Moreover, the values of MVL_{Max} were significantly larger for LEC than MEC (LEC median = 0.35, MEC median = 0.22; Wilcoxon rank-sum test, z = 4.73, $P = 2.21 \times 10^{-6}$, LEC, n = 72, MEC, n = 117) (Fig. 1L).

We next investigated whether LEC cells could encode the egocentric bearing of discrete, external items when a rat foraged in an arena that contained four objects (Fig. 2A and fig. S1, C and D) (*16*). We first determined which one of the four objects for each cell generated the strongest egocentric bearing tuning (largest MVL). LEC cells had a significant preference for egocentric representation of those objects ($\Delta BIC_{Object} < 0$), whereas MEC cells preferred the allocentric representation ($\Delta BIC_{Object} > 0$) (LEC median = −0.0026; MEC median = 0.0011; Wilcoxon signed-rank test; LEC: z = −8.13, $P = 4.41 \times 10^{-16}$, n = 140; MEC: z = 3.97, $P = 7.08 \times 10^{-5}$, n = 88; LEC vs. MEC: Wilcoxon rank-sum test, z = −8.35, $P = 6.85 \times 10^{-17}$) (Fig. 2, B and C; figs. S11 and S12; and table S4).

To investigate whether LEC cells represented the locations of each object in the rat's immediate vicinity as it explored, we partitioned the box into sections based on the closest object to each location in the box (Fig. 2D and fig. S11B). Using the data in each partition, we constructed the MVL map to search for the MVL_{Max} location in the entire arena (Fig. 2D) and computed the egocentric bearing tuning of the object in that partition ($Bearing_{Object}$) (Fig. 2E and fig. S13). An object-representing partition was defined as a partition in which the MVL of $Bearing_{Object}$ was >0.25 and the MVL map showed a small, localized peak (less than 20% of the arena with values >70% of the peak value) close to the local object (<25 cm). For the cells with two or more object-representing partitions, the preferred $Bearing_{Object}$ values across the partitions were significantly more similar to each other for LEC cells than for MEC cells (Fig. 2F) (Rayleigh test: LEC, z = 12.15, $P = 1.42 \times 10^{-7}$, n = 15; MEC, z = 0.51, P = 0.62, n = 8; absolute value: LEC median = 18.26°, MEC median = 114.35°; LEC vs. MEC, Wilcoxon rank-sum test, z = −3.58, $P = 3.40 \times 10^{-4}$), indicating a more

[1]Zanvyl Krieger Mind/Brain Institute, Johns Hopkins University, Baltimore, MD, USA. [2]Centre for Neuroscience, Indian Institute of Science, Bangalore, India. [3]National Brain Research Centre, Haryana, India. [4]Solomon H. Snyder Department of Neuroscience, Johns Hopkins University, Baltimore, MD, USA.
*These authors contributed equally to this work. †Corresponding author. Email: jknierim@jhu.edu

reliable egocentric code for objects in LEC than MEC (figs. S11D and S12B).

To determine whether behaviorally salient locations were represented in an egocentric framework, we recorded LEC cells in a goal-oriented task (Fig. 3A and fig. S1E), in which the goal (a food well) was shifted between sessions. Food pellets were thrown sporadically into the food well and other places in the box, encouraging both exploration of the entire box and frequent visits to the goal (Fig. 3B). Some cells encoded the egocentric bearing of the goal [current goal locations (Fig. 3C) and standard goal location (Fig. 3D); see also fig. S14]. The standard goal quadrant (southeast) was overrepresented compared to the northeast quadrant, which never contained a goal location (Monte Carlo test against a uniformly distributed random distribution, $P < 0.002$ for all three sessions) (Fig. 3E). Between sessions, there was a significant change in the number of cells that represented the standard versus displaced goal locations (bootstrap test, $P < 0.01$ for both S1 vs. S2 and S2 vs. S3) (Fig. 3E), which could not be explained by behavioral confounds at the goal location (fig. S15). As in the first experiment, some cells also showed distance selectivity to the MVL_{Max} location (fig. S16 and table S5).

These results demonstrate that LEC represents the bearing of external items in an egocentric framework. They confirm a key prediction of the hypothesis, that the LEC provides the hippocampus with the sensory input that constitutes the content of an episodic memory (*7*, *8*, *16*, *17*). They are also consistent with an earlier hypothesis that, in contrast to the MEC representation of "self" location, LEC mainly represents information of "other" items in an egocentric framework (*9*). Findings in rats, bats, and primates have highlighted the involvement of the hippocampus in such representations of "other" (*14*, *18*–*22*). We suggest that the LEC provides information about items in the environment, which is used for building comprehensive maps of what is "out there" (*9*, *21*, *22*). This functional segregation of "self" information in MEC and "other" information in LEC may reflect a fundamental organizing principle of the medial temporal lobe memory system (*7*, *9*).

Spatial information in the hippocampal formation is generally considered to be represented in an allocentric framework. However, the present findings revealed that LEC cells displayed a robust spatial representation in an egocentric framework. Thus, LEC provides an integration of spatial and nonspatial information, in the form of a spatial relationship between the observer

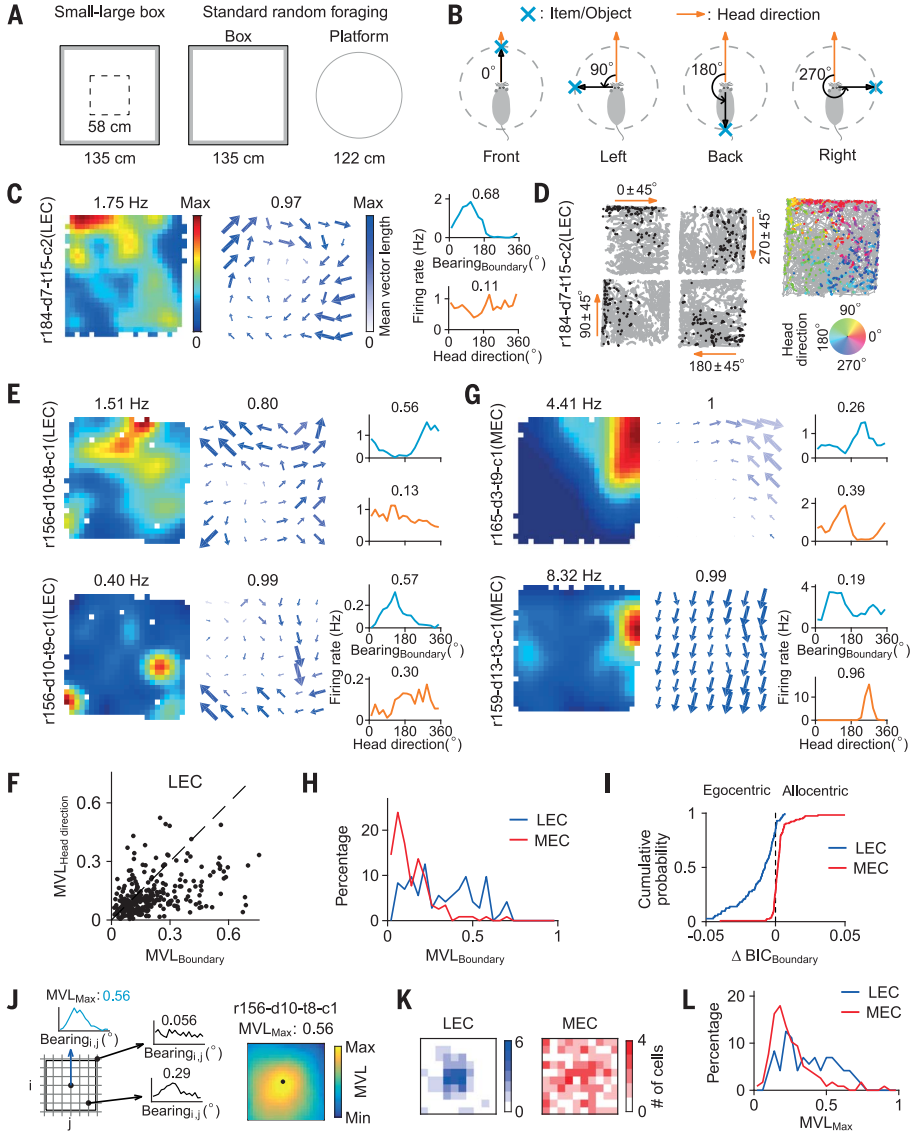

Fig. 1. LEC but not MEC cells show egocentric bearing tuning of nearby boundaries in open arenas. (**A**) Experimental setups. In some experiments (small-large box), rats foraged first in a small box and then the inner walls were removed to allow the rat to forage in the large box. In other experiments, rats foraged either in a square box or a circular platform. (**B**) Definition of egocentric bearing, the angle of the vector (black) from the rat to an external item (cyan), in reference to the rat's allocentric head direction (orange). (**C**) Example of an LEC cell. (Left) Spatial rate map (number on top denotes the peak firing rate). (Middle) Head direction tuning field plot showing preferred head direction (arrow direction) at different locations. Arrow size denotes firing rate. Color saturation denotes the MVL of the tuning curve. Number on top, maximum MVL. (Right) Tuning curves of egocentric bearing of the boundary (top) and allocentric bearing (i.e., classic head direction) (bottom). Number on top is the MVL. (**D**) Same cell as shown in panel C. (Left four panels) The trajectory (gray line) and position of the rat when the cell fired (black dots), separated based on the current head direction. (Right) Overall trajectory; dot color signifies head direction. (**E**) A pair of simultaneously recorded cells showing opposite preferred $Bearing_{Boundary}$ values. (**F**) Scatter plot of MVLs for allocentric head direction tuning vs. $Bearing_{Boundary}$ tuning. (**G**) Two examples of MEC cells (see additional description in the caption for fig. S8B). (**H**) Distributions of MVLs of $Bearing_{Boundary}$ tuning curves of LEC and MEC cells. (**I**) Cumulative distributions of $\Delta BIC_{Boundary}$ values for LEC and MEC cells. (**J**, left) Schematic of MVL map construction. Tuning curves of egocentric bearing of each location (coordinates *i*, *j*) were constructed; the values of the MVL for each location were plotted. (Right) Example of an MVL map with the location of the peak (MVL_{Max} location) denoted with a black dot. (**K**) 2D histograms of the distributions of MVL_{Max} locations for LEC and MEC cells in the small-large box task. Overrepresentation of the arena center corresponds to overrepresentation of the environmental boundaries (fig. S2A). (**L**) Distributions of MVL_{Max} values for LEC and MEC cells.

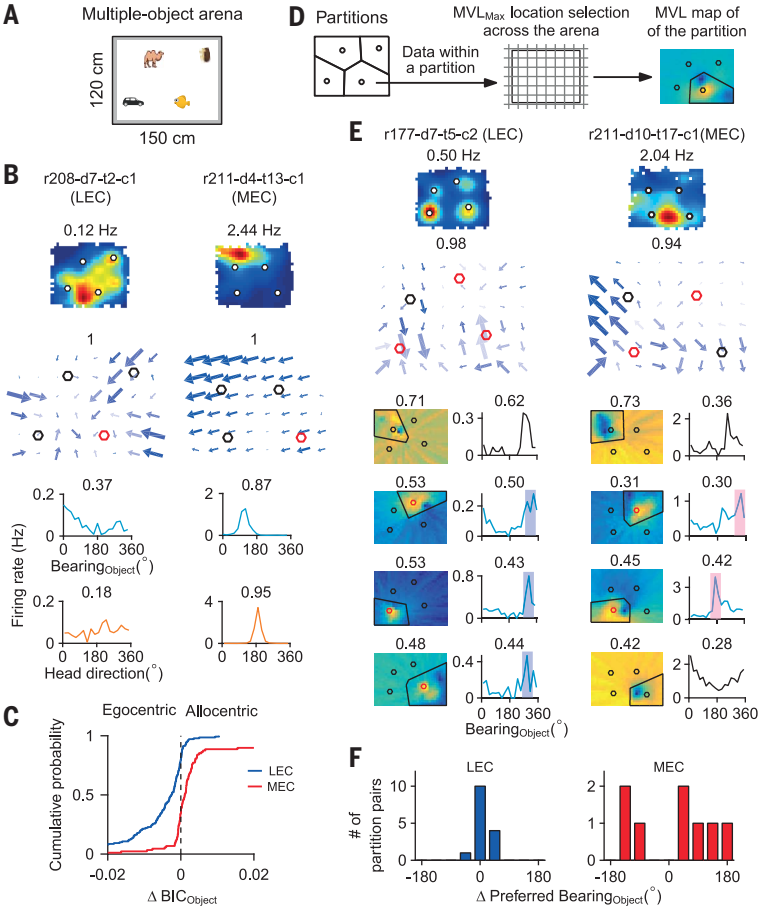

Fig. 2. LEC but not MEC cells show egocentric bearing tuning of 3D objects. (**A**) The multiple-object arena. (**B**) Example cells from LEC (left column) and MEC (right column). Top to bottom, spatial rate map (circles denote the objects), head direction tuning field plot (red circle denotes the object with the highest MVL_{Object}), egocentric bearing tuning curve for the object with the highest MVL_{Object}, head direction tuning curve. (**C**) Cumulative distributions of best ΔBIC_{Object} values for LEC and MEC cells. (**D**) Schematic showing construction of an MVL map with data in a local partition. (**E**) Examples of cells from LEC (left) and MEC (right) with multiple object-representing partitions. (Top to bottom) Spatial rate map, head direction tuning field plot, and MVL maps, together with tuning curves of egocentric bearing of the local object for four partitions. Colored tuning curves were constructed from object-representing partitions (the partitions with red circles denoting the object), which are the ones with a sharp peak near the local object on the MVL map. Note that the preferred bearings (shaded regions) of the LEC cell were consistent, whereas the MEC cell had different preferred bearings for each object. (**F**) Distributions of the differences in preferred $Bearing_{Object}$ values between object-representing partition pairs for LEC and MEC cells with more than one object-representing partition.

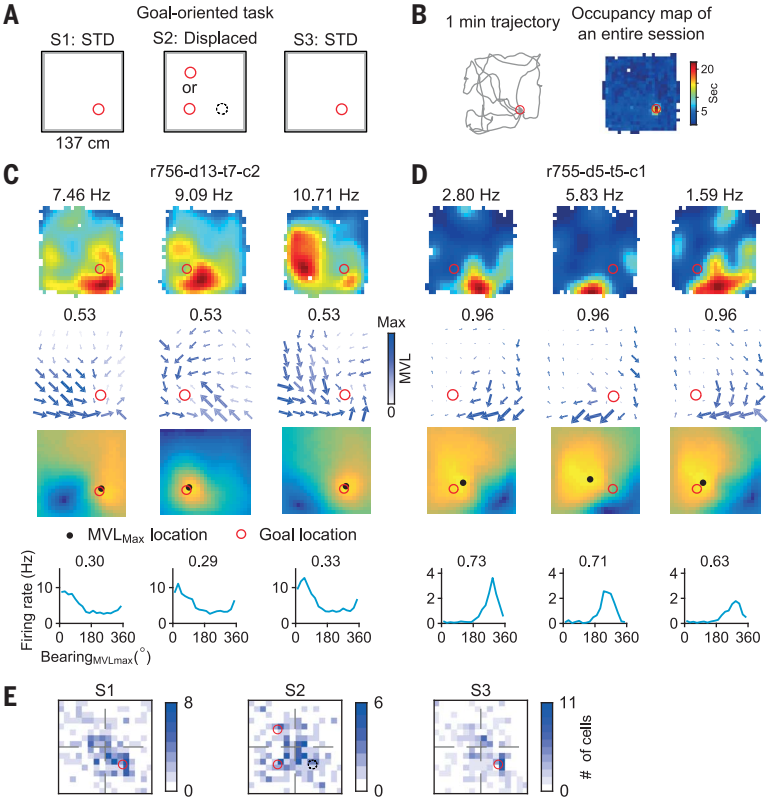

Fig. 3. LEC cells show goal-related egocentric tuning. (**A**) The goal-oriented task. A single food well (red circle) was shifted from the standard goal location (STD) in session 1 to one of two displaced locations in session 2, and then back to the original standard location in session 3. (**B**, left) Typical trajectory of rats in this task for 1 min. (Right) Typical occupancy map in an entire session. The goal location is overoccupied. (**C**) An example cell in three sessions (columns). (Top to bottom) Spatial rate maps, head direction tuning field plots, MVL maps (red circle, food well), and egocentric bearing tuning curves for MVL_{Max} locations. The MVL_{Max} locations for this neuron coincided with the current goal location in each session, as shown in the MVL maps. (**D**) Another example cell. The standard goal location was represented on the MVL maps regardless of the current goal locations. (**E**) 2D histograms of the distributions of MVL_{Max} locations in three sessions.

and specific items in the world, which deviates from the conventional view that spatial ("where") information is conveyed only through the postrhinal (parahippocampal)-MEC pathway (*7*, *8*). These results also clarify the interpretation of recent lesion studies of the entorhinal cortex. First, LEC is critical for performance of an object-place association task that promotes the use of an egocentric strategy (*23*); second, hippocampal cells in rats with a complete lesion of MEC still had place fields, which suggests that input from LEC alone can support hippocampal spatial selectivity (*24*) through transformation of egocentric direction and distance information, as proposed in some of the earliest models of place cells (*25*, *26*). It is thus likely that LEC contributes to the process of abstraction of egocentric information into an allocentric framework for memory storage (*5*, *12*). The parietal cortex is often viewed as an essential node in providing limbic system structures with egocentric representations of cues (*13*) and actions (*27*, *28*) for memory and navigation (*29*), but it is assumed that the information must undergo a transformation from egocentric to allocentric coordinates (*29*) before reaching the hippocampus. However, at least in rats, the LEC receives direct projections from the parietal cortex (*30*), thus allowing the hippocampus to combine directly these egocentric representations from the parietal cortex with the MEC allocentric representations of self-position.

REFERENCES AND NOTES

1. W. B. Scoville, B. Milner, *J. Neurol. Neurosurg. Psychiatry* **20**, 11–21 (1957).
2. L. R. Squire, *Neurobiol. Learn. Mem.* **82**, 171–177 (2004).
3. F. Vargha-Khadem *et al.*, *Science* **277**, 376–380 (1997).
4. M. A. Conway, *Neuropsychologia* **47**, 2305–2313 (2009).
5. J. O'Keefe, L. Nadel, *The Hippocampus as a Cognitive Map* (Oxford: Clarendon Press, 1978).
6. E. I. Moser, M.-B. Moser, B. L. McNaughton, *Nat. Neurosci.* **20**, 1448–1464 (2017).
7. J. J. Knierim, J. P. Neunuebel, S. S. Deshmukh, *Philos. Trans. R. Soc. Lond. B Biol. Sci.* **369**, 20130369 (2013).
8. H. Eichenbaum, A. P. Yonelinas, C. Ranganath, *Annu. Rev. Neurosci.* **30**, 123–152 (2007).
9. J. E. Lisman, *Prog. Brain Res.* **163**, 615–625 (2007).
10. E. L. Hargreaves, G. Rao, I. Lee, J. J. Knierim, *Science* **308**, 1792–1794 (2005).
11. D. Yoganarasimha, G. Rao, J. J. Knierim, *Hippocampus* **21**, 1363–1374 (2011).
12. A. Peyrache, N. Schieferstein, G. Buzsáki, *Nat. Commun.* **8**, 1752 (2017).
13. A. A. Wilber, B. J. Clark, T. C. Forster, M. Tatsuno, B. L. McNaughton, *J. Neurosci.* **34**, 5431–5446 (2014).
14. A. Sarel, A. Finkelstein, L. Las, N. Ulanovsky, *Science* **355**, 176–180 (2017).
15. Materials and methods are available as supplementary materials.
16. S. S. Deshmukh, J. J. Knierim, *Front. Behav. Neurosci.* **5**, 69 (2011).
17. A. Tsao, M.-B. Moser, E. I. Moser, *Curr. Biol.* **23**, 399–405 (2013).
18. E. T. Rolls, S. M. O'Mara, *Hippocampus* **5**, 409–424 (1995).
19. N. J. Killian, M. J. Jutras, E. A. Buffalo, *Nature* **491**, 761–764 (2012).
20. L. Acharya, Z. M. Aghajan, C. Vuong, J. J. Moore, M. R. Mehta, *Cell* **164**, 197–207 (2016).
21. T. Danjo, T. Toyoizumi, S. Fujisawa, *Science* **359**, 213–218 (2018).
22. D. B. Omer, S. R. Maimon, L. Las, N. Ulanovsky, *Science* **359**, 218–224 (2018).
23. D. I. G. Wilson, S. Watanabe, H. Milner, J. A. Ainge, *Hippocampus* **23**, 1280–1290 (2013).
24. J. B. Hales *et al.*, *Cell Reports* **9**, 893–901 (2014).
25. J. O'Keefe, *Hippocampus* **1**, 230–235 (1991).
26. P. E. Sharp, *Psychobiology* **19**, 103–115 (1991).
27. B. L. McNaughton *et al.*, *Cereb. Cortex* **4**, 27–39 (1994).
28. J. R. Whitlock, G. Pfuhl, N. Dagslott, M.-B. Moser, E. I. Moser, *Neuron* **73**, 789–802 (2012).
29. P. Byrne, S. Becker, N. Burgess, *Psychol. Rev.* **114**, 340–375 (2007).
30. G. M. Olsen, S. Ohara, T. Iijima, M. P. Witter, *Hippocampus* **27**, 335–358 (2017).

ACKNOWLEDGMENTS

The authors thank G. Rao, A. Smolinsky, and M. Lee for technical assistance and A. Tsao for critical reading of the manuscript. **Funding:** This work was supported by NIH grant R01 MH094146, NIH grant R01 NS039456, and the International Human Frontier Science Program Organization LT00683/2006C (F.S.). **Author contributions:** C.W. and J.J.K. conceived and designed the study. C.W., X.C., H.L., S.S.D., Y.D., and F.S. performed the experiments. C.W. and X.C. performed the data analyses. J.J.K. supervised the experiments and analyses. C.W., X.C., and J.J.K. wrote the paper with inputs from all authors. **Competing interests:** None declared. **Data and materials availability:** Data and code are accessible at https://sites.krieger.jhu.edu/knierim-lab/resources/data-for-wang-chen-et-al/.

SUPPLEMENTARY MATERIALS

www.sciencemag.org/content/362/6417/945/suppl/DC1
Materials and Methods
Figs. S1 to S16
Tables S1 to S5
References (*31*–*39*)

15 June 2018; accepted 19 October 2018
10.1126/science.aau4940

Science

Egocentric coding of external items in the lateral entorhinal cortex

Cheng Wang, Xiaojing Chen, Heekyung Lee, Sachin S. Deshmukh, D. Yoganarasimha, Francesco Savelli and James J. Knierim

Science **362** (6417), 945-949.
DOI: 10.1126/science.aau4940

Egocentric representation of objects

The lateral entorhinal cortex (LEC) and medial entorhinal cortex (MEC) are the two major cortical projections to the hippocampus. The discovery of a variety of functional cell types in MEC has greatly advanced our understanding of the functional anatomy of entorhinal-hippocampal circuits. However, the function of LEC and the behavioral correlates of LEC cells are still not fully understood. Wang *et al.* analyzed the firing properties of LEC and MEC neurons. They found that LEC and MEC used different reference frames, with LEC encoding objects egocentrically.

Science, this issue p. 945